

Long-Lived Nuclear Coherences inside Helium Nanodroplets

Bernhard Thaler¹, Miriam Meyer¹, Pascal Heim, and Markus Koch^{1*}*Graz University of Technology, Institute of Experimental Physics, Petersgasse 16, 8010 Graz, Austria* (Received 26 August 2019; accepted 6 February 2020; published 20 March 2020)

Much of our knowledge about dynamics and functionality of molecular systems has been achieved with femtosecond time-resolved spectroscopy. Despite extensive technical developments over the past decades, some classes of systems have eluded dynamical studies so far. Here, we demonstrate that superfluid helium nanodroplets, acting as a thermal bath of 0.4 K temperature to stabilize weakly bound or reactive systems, are well suited for time-resolved studies of single molecules solvated in the droplet interior. By observing vibrational wave packet motion of indium dimers (In_2) for tens of picoseconds, we demonstrate that the perturbation imposed by this quantum liquid can be lower by a factor of 10–100 compared to any other solvent, which uniquely allows us to study processes depending on long nuclear coherence in a dissipative environment. Furthermore, tailor-made microsolvation environments inside droplets will enable us to investigate the solvent influence on intramolecular dynamics in a wide tuning range from molecular isolation to strong molecule-solvent coupling.

DOI: [10.1103/PhysRevLett.124.115301](https://doi.org/10.1103/PhysRevLett.124.115301)

A comprehensive understanding of mechanisms to convert solar energy into other energy forms is a prime objective for many research fields, with potential impact on light harvesting applications or the modeling of photoprotection in biomolecules. Insight into the functionality and dynamics of photoactive systems can be obtained in a unique way with time-resolved laser spectroscopy [1], revealing information about, for example, nonadiabatic coupling dynamics of electrons and nuclei [2], charge transfer [3], electron dynamics [4], or molecular chirality [5]. Recent experiments on technologically and biophysically relevant molecules suggest that nuclear motions and in particular their coherences have strong influence on the electronic evolution of the system [6]; examples include prototypical molecules for photosynthesis [7–9] and photovoltaics [10], or metal-halide perovskites [11,12]. The evolution of a molecular system after photoexcitation strongly depends on its immediate environment, with significant differences between isolated systems, where photodynamics can be precisely studied [13,14], and the system in its real-world environment in the condensed phase. Isolated molecules can be produced in a seeded supersonic expansion [15], where investigations are, however, often prevented by fragmentation resulting from excess energy during photoexcitation, or simply by the fact that weakly bound systems cannot be produced. This harmful vibrational energy can be dissipated to a thermal bath by embedding molecules in a high-pressure buffer gas [16] or a cryogenic matrix [17]. As a disadvantage, influences of the environment on intrinsic dynamics can be severe and disentangling intra- and intermolecular dynamics is often impossible. Moreover, in such environments molecular dynamics cannot be probed with time-

resolved photoelectron (PE) or photo-ion spectroscopy [13,14], two very powerful methods that are independent of selection rules and dark states. Because of these drawbacks, many systems have eluded ultrafast studies.

Here we demonstrate that superfluid helium nanodroplets (He_N) are well suited to fill this gap. By tracing vibrational dynamics of fully solvated molecules for the first time, we show that superfluid He as a solvent can have very little influence on the coherence of nuclear dynamics. Our results also demonstrate that time-resolved PE spectroscopy is a proper method to observe the dynamics of solvated molecules. The benefits of He_N for spectroscopy have been unveiled over the last three decades [18,19]: these nanometer-sized quantum fluid containers have enabled researchers to produce, isolate, and investigate, for example, fragile agglomerates [20,21], tailor-made complexes [22,23], highly reactive species [24], or molecules in a controlled microsolvation environment [25]. Femtosecond time-resolved investigations of He_N , building on pioneering works in bulk superfluid He [26], have recently moved into the focus of researchers and various studies have been presented, including pure droplets [27], alkali-metal atoms and molecules located on the droplet surface [28–30], as well as alignment [31] and rotational studies [32]. While vibrational dynamics for alkali-metal dimers on the droplet surface were found to exhibit weak or very weak perturbations [33–35], the influence on fully solvated species in the droplet interior is generally stronger [19], which might lead to complete suppression of intramolecular dynamics [36]. In the presented experiments we investigate vibrational wave packet (WP) motion of single In_2 molecules located inside He droplets. We find that the decay of the WP signal is surprisingly low, which enables

us to quantify the influence of the quantum fluid on nuclear coherence.

The setup is described in detail elsewhere [37,38]. In short, He_N with a mean droplet size of about 9000 atoms are generated via supersonic expansion of high purity helium gas through a cryogenic nozzle (5 μm diameter, 15 K temperature, 40 bar stagnation pressure) into vacuum. The droplets are loaded with, on average, two In atoms by a resistively heated indium oven, resulting in In_2 molecules solvated in the droplet interior. We investigate the $\text{In}_2 - \text{He}_N$ system with femtosecond time-resolved photoelectron spectroscopy using pulses from an amplified Ti:sapphire laser system (800 nm center wavelength, 25 fs duration, 4.2 mJ pulse energy, 3 kHz repetition rate). Pump pulses are frequency up-converted by combining optical parametric amplification and subsequent frequency quadrupling to 345 nm (3.60 eV, 70 meV FWHM), in order to excite In_2 at the maximum of the in-droplet $\text{B}^3\Pi_g \leftarrow \text{X}^3\Pi_u$ transition band (see Supplemental Material, Note 1 [39]). Probe pulses are frequency doubled to 406 nm (3.05 eV, 40 meV FWHM) in a 1 mm thick BBO crystal. Pulse energies of (2.2 ± 0.5) and (4.0 ± 0.5) μJ are used for pump and probe pulses, respectively. Pulses are focused into the measurement chamber with a 1000 mm lens, the cross correlation based on the In_2 overlap signal is estimated to be below 250 fs. PE kinetic energies and ion charge-to-mass ratios are measured in a time-of-flight spectrometer.

Photoexcitation of the $\text{In}_2 - \text{He}_N$ system triggers two different types of dynamics: The response of the He solvation shell [Fig. 1(a)] and a vibrational WP in In_2 [Fig. 1(b)]. Both dynamics are represented in the transient PE spectra with overlapping timescales (Fig. 2) and we identify the solvation shell response by comparison with the In atom transient, which is described in our previous work [37]. Ground state atoms and molecules inside He_N reside in cavities termed bubbles due to Pauli repulsion

between the dopant's valence electrons and the closed shell He atoms. Photoexcitation and the correlated expansion of the valence orbital leads to an increase of the bubble size [Fig. 1(a)]. For In_2 , the connected transfer of potential energy to He kinetic energy is observed as shift of the PE peak from about 0.75 to 0.60 eV within the first picosecond [Fig. 2(b)]. In the excited state, In_2 is ejected from the droplet, which can be deduced from the transient In_2^+ ion yield [red line in Fig. 2(a)]. Following absent ion signals for the first 50 ps, the ion yield shows a slow rise within 200 ps because ionization of In_2 inside or in the vicinity of the droplet leads to trapping of the ion, preventing In_2^+ detection [28,29].

We now turn to the intramolecular In_2 WP dynamics. Photoexcitation with a spectrally broad femtosecond laser pulse leads to coherent superposition of several vibrational eigenfunctions and the periodic movement of the resulting WP is detected as modulation of the PE signal [Fig. 1(b)]. This modulation with a periodicity of 0.42 ps is clearly seen in the time-resolved PE spectrum [Fig. 2(b)], as well as the integrated PE yield [Fig. 2(e)]. Anharmonicity of the potential leads to dispersion of the eigenfunctions and a spreading of the WP, detected as decrease of the modulation contrast [Fig. 2(e)]. The reversible character of dispersion leads to refocusing of the WP at characteristic revival times, restoring the signal contrast to some extent. Half and full revivals of the In_2 motion are indeed observed around 145 ps [Figs. 2(c) and 2(f)] and 290 ps [Figs. 2(d) and 2(g)], respectively; the assignment stems from a comparison to the theoretical revival time, which is based on the anharmonicity parameter of the Morse potential (see Supplemental Material, Note 1 [39]). The reduced amplitude in the revival signal, compared to the initial oscillation, reflects decoherence (dephasing) of the WP due to molecule-He interaction. Note that the full revival around 290 ps is observed at times where all excited dimers have left their droplets, as indicated by the leveling off of the In_2^+

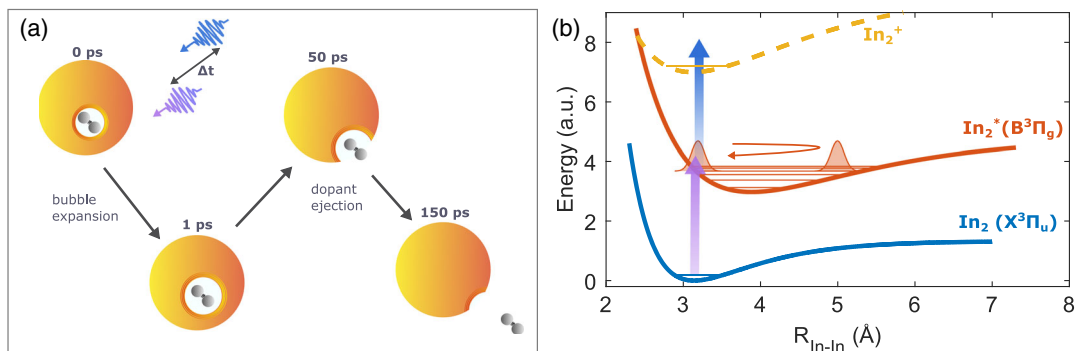


FIG. 1. Schematic drawing of the photoinduced dynamics of the $\text{In}_2 - \text{He}_N$ system. (a) Solvent response: Expansion of the He solvation shell (bubble) during the first picosecond is followed by In_2 ejection within about 100 ps. (b) Intramolecular In_2 dynamics: A coherent superposition of vibrational states is generated by the spectrally broad pump pulse, leading to vibrational WP motion in the excited molecule. The WP is probed with a second pulse, resulting in a modulation of the photoelectron or photo-ion yield due to an alternating ionization probability. Ground and excited state Morse potentials were taken from Ref. [46], the shape of the ionic potential is not known and therefore only schematically drawn.

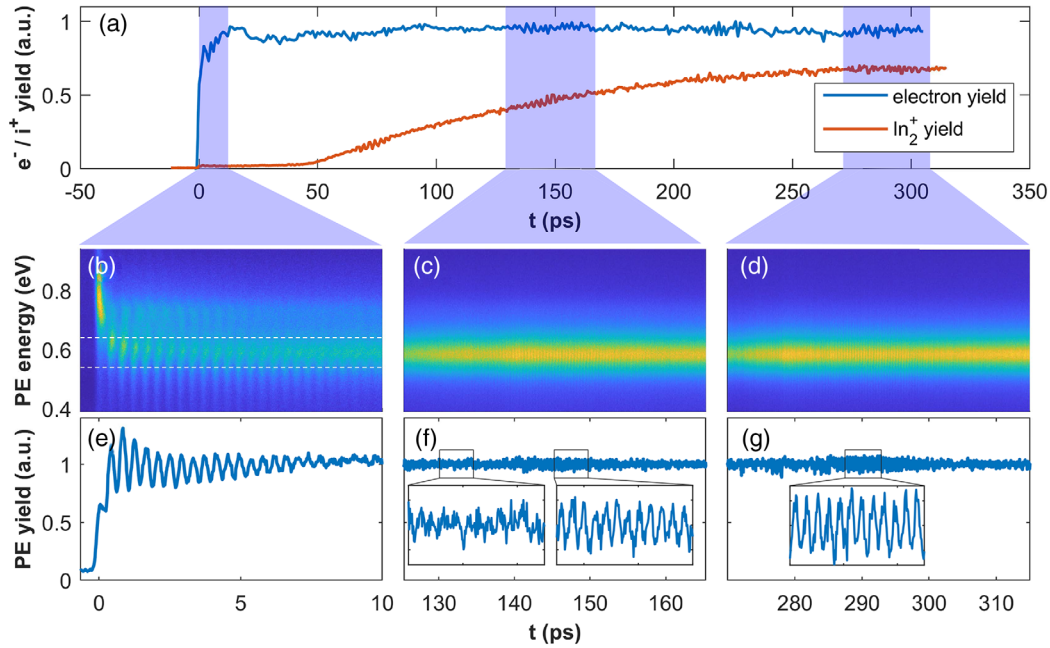


FIG. 2. Photoelectron and photo-ion transients representing the dynamics of the $\text{In}_2 - \text{He}_N$ system. (a) Transient PE (blue) and In_2^+ (red) ion yields. (b) to (d) PE kinetic energy spectrum as a function of pump-probe delay for temporal regions of the initial WP signal (b), as well as the first half (d) and full (d) revival, respectively; dashed lines mark the integration region. (e) to (g) Integrated PE signal for the energy region 0.54 to 0.64 eV, containing close-ups of the half and full revival to better visualize the oscillating signals. Integrated curves are normalized to their sliding average (2.5 ps window), in order to compensate for long-term laser drifts.

ion signal [Fig. 2(a)]. As expected, the next revival (3/2) can be observed around 435 ps, exhibiting the same oscillation contrast and temporal amplitude characteristics (see Supplemental Material, Note 4 [39]). The fact that fractional revivals (quarter: ~ 70 ps, half: ~ 145 ps) and full revivals (~ 290 ps) are also observed in the In_2^+ yield [Fig. 2(a)], whereas they are absent during the initial oscillation, proves that the WP signals are associated to In_2 molecules that are originally solvated inside the droplet (see Supplemental Material, Note 2 [39]).

Fourier transformation of the three datasets shown in Figs. 2(b)–2(d) reveals always the same central frequency of (2.42 ± 0.05) THz, corresponding to an oscillation period of (0.42 ± 0.01) ps. To obtain insight into the transient changes of the oscillating signals, we apply sliding window Fourier analysis (see Supplemental Material, Note 3 [39]). Figures 3(a)–3(c) show the three spectrograms corresponding to the initial WP oscillation, the half revival and the full revival, respectively. The transient amplitudes of the central frequency are shown

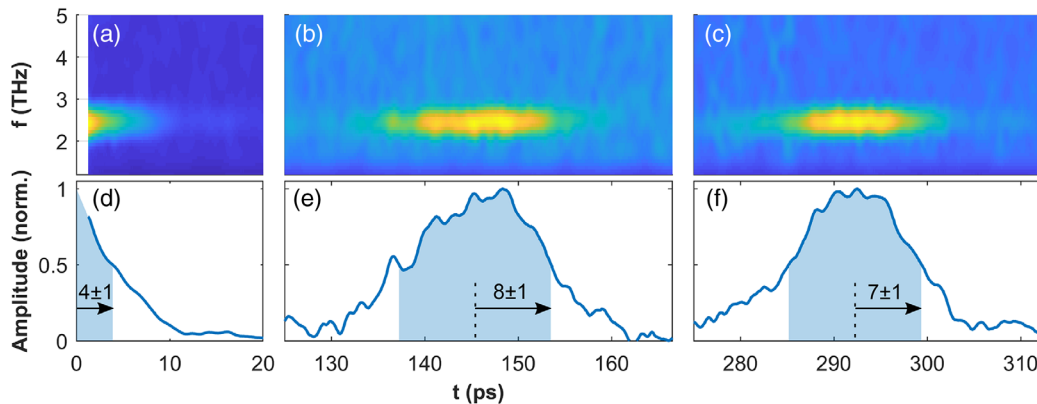


FIG. 3. Sliding window fast Fourier analysis of the WP signals shown in Figs. 2(b)–2(d). A Hamming window function of 2.5 ps width was used (see Supplemental Material, Note 3 [39]), resulting in a spectral width of 0.55 THz (FWHM). (a) to (c): Spectrograms, for which the PE energy range between 0.49 and 0.64 eV was considered. (d) to (f): Time-dependent amplitudes of the central frequency (2.42 THz). Arrows indicate the time after which the signal has decreased to 50% of its maximum value [for the extrapolation to 0 ps in panel (d), see Supplemental Material, Note 3 [39]].

in Figs. 3(d)–3(f), revealing that the signal amplitude of the initial WP oscillation [Fig. 3(d)] decreases faster than the amplitudes of the half and full revivals [Figs. 3(e) and 3(f)]. The same frequency for In₂ inside and outside the He_N hints at a minor influence of the helium solvent on the shape of the excited state potential. Upward-bent potentials, as observed for halogens in rare gas matrices [17], might however still influence WP motion at higher vibrational energies.

We now further analyze the time- and frequency-domain representations of the WP motion. The persistent strong oscillation signals within the first 10 ps [Figs. 2(e) and 3(d)], as well as the appearance of WP revivals [Figs. 2(f) and 2(g) and Figs. 3(e) and 3(f)] show that coherence is conserved to some degree inside He_N. Since the full revival occurs after the molecules are ejected from the droplet, comparison of the oscillation signal decay times for solvated and free molecules is possible and provides insight into the He-induced decoherence. Solvated In₂ experience both dispersion and He-induced decoherence of the WP, resulting in a 50% decrease of the oscillation amplitude within (4 ± 1) ps [Fig. 3(d)]. Free In₂, in contrast, experience only dispersion, leading to a slower decrease of about (8 ± 1) ps [Figs. 3(e) and 3(f)]. We thus estimate a decoherence half-life caused by He interaction on the order of ~ 10 ps. Let us note that a slower decrease of the oscillation amplitude due to dispersion could be reached by a reduction of laser bandwidth. We have, however, refrained from this possibility, as the accompanying increase in pulse duration would lead to a reduction in oscillation contrast. From the estimated decoherence time a lower limit for the duration of the In₂ ejection can be estimated. The oscillation contrast at the peak of the revivals is roughly 20% of its initial value after photoexcitation [Figs. 2(e)–2(g)]. Assuming an exponential-like decrease, we estimate that the In₂ molecule is surrounded by He for about 20 ps, corresponding to twice the decoherence time. This interpretation is in line with the absent ion yield within the first 50 ps [Fig. 2(a)], taking into account that the ejected In₂ has to move a certain distance from the droplet surface to avoid recapture by the droplet upon ionization [28,29]. We note that the revivals could, in principle, also be related to In₂ molecules that are ejected earlier than 20 ps after excitation, which seems very unlikely in view of the ion yield onset at 50 ps. However, this scenario would not change the observation of coherent oscillations lasting for over 20 ps, which is purely based on the initial oscillation contrast decay. In general, the slow ion yield increase within 200 ps, reflecting the spatial distribution inside the droplet in combination with the droplet size distribution, suggests that the vast majority of In₂ undergoes much longer He interaction than 20 ps. In this case, the decoherence time would be significantly shorter than the average In₂ ejection time, pointing towards a nonconstant, time-dependent loss of phase information; the vibrational WP dephases more strongly within the first few picoseconds after photoexcitation.

Because the vibrational motion of In₂ is started at short internuclear distances [see Fig. 1(b)], one might expect strong energy transfer to the droplet during the first half oscillation period of 0.21 ps, as the atoms hit the solvation shell boundary. However, the photoexcitation-induced expansion of this shell takes also place within the first few hundred femtoseconds; the He boundary layer moves therefore at a similar pace as the separating In atoms, relativizing this assumption. A possible explanation for stronger initial He influence might be found in helium density waves, which are initiated by the bubble expansion and reflected by the droplet surface to interact with the molecule after a few ps [37]. Subsequent to this relatively strong initial interaction, decoherence during the molecule's propagation through the droplet seems to be much weaker. Even dopant ejection does not destroy the vibrational phase relations, despite possible recoil effects when the molecule ruptures the droplet boundary.

Coherence decay can be caused in two ways: (i) pure dephasing of the vibrational modes (elastic dephasing), or (ii) vibrational relaxation within the In₂ excited electronic potential, resulting in energy transfer from the molecule to the droplet (inelastic dephasing). As phase-conserving vibrational relaxation would lead to a WP frequency increase [47], which is not observed in our case [Figs. 3(a)–3(c)], we can conclude that for In₂ either solely elastic dephasing, or elastic dephasing in combination with noncoherent vibrational relaxation are present.

Viewing the In₂ and the He bubble as two quantum oscillators that are only weakly coupled because of their different excitation energies further suggests a low influence of the He surrounding: In₂ has a much larger excitation energy of 80 cm^{-1} (0.42 ps oscillation period) compared to 1.1 cm^{-1} (30 ps) of the He bubble [37]. Apart from the bubble, the In₂ motion might also couple to the droplet's elementary excitations, which can be grouped in bulk excitations (phonons) and surface excitations (ripples) [48]. Whereas ripples should only weakly couple to the molecular vibration due to their small energies (below 1 cm^{-1}), phonons can have energies on the order of 10 cm^{-1} , which is closer to the energy spacing of In₂ vibrations. Experiments on molecules with high vibrational energy spacing (HF, 2000 cm^{-1}) showed no relaxation within at least 0.5 ms [22], whereas simulations for I₂ excited to low vibrational states inside He_N predict time-scales down to a few hundred picoseconds [49], for a vibrational energy spacing of around 200 cm^{-1} . Based on these results, we conclude that the In₂ spends insufficient time within the droplet in order to experience substantial vibrational relaxation.

The low perturbing character of superfluid He as a quantum solvent becomes especially clear when the observed long-lasting vibrational coherences of tens of ps are compared to other solvents, where coherence loss typically proceeds within some hundred femtoseconds up to a few picoseconds in special cases [50]. Even in cryogenic rare-gas matrices decoherence times are limited

to few picoseconds [17]. For alkali-metal dimers on He_N , which reside on the droplet's surface, a range of weak decoherence (~ 1.5 ns) [33,34] to strong decoherence (~ 5 ps) [35] was observed. Given the pronounced blueshift of the electronic transition that launches the WP in solvated In_2 , the observation of low decoherence is remarkable.

The preservation of nuclear coherence inside He_N will be particularly important for systems with processes that are dominated by coherent nuclear motion [6], such as prototypical systems for photosynthesis [7–9] and photovoltaics [10]. Because of their confinement character, He_N are able to isolate single donor-acceptor pairs of light-harvesting complexes [51]. The generation of controlled microsolvation environments inside He_N will allow us to follow the transition from dynamics of isolated molecules in He_N to the interaction-dominated behavior of solvated systems by successively adding solvent molecules [25].

In a general perspective, all dynamical studies in a dissipative environment face the problem that on the one side, coupling to a thermal bath is required to dissipate energy, while on the other side, transition states of chemical reactions are generally prone to increased solvent interaction as they are associated with large amplitude nuclear movements. Our results indicate that the strongly reduced influence of superfluid He might allow us to follow transition state dynamics in many systems that were previously inaccessible. Coupling to the solvent depends on many aspects, such as the molecule's vibrational energy, the character of the vibrational mode, or the excited state electronic structure. More complex molecular systems are expected to couple more strongly to the He solvent; examples include molecules with permanent dipole moments, electronic states with ionic character, or low-frequency vibrational modes, all of which will be interesting to study in the future.

We thank Wolfgang E. Ernst for providing the laser system and fruitful discussions, Leonhard Treiber for experimental support, and Martin Schultze for reading the manuscript. We acknowledge financial support by the Austrian Science Fund (FWF) under Grant No. P29369-N36, as well as support from NAWI Graz.

* markus.koch@tugraz.at

- [1] A. H. Zewail, Femtochemistry: Atomic-scale dynamics of the chemical bond, *J. Chem. Phys. A* **104**, 5660 (2000).
- [2] Y. Kobayashi, K. F. Chang, T. Zeng, D. M. Neumark, and S. R. Leone, Direct mapping of curve-crossing dynamics in IBr by attosecond transient absorption spectroscopy, *Science* **365**, 79 (2019).
- [3] C. Consani, G. Auböck, F. van Mourik, and M. Chergui, Ultrafast tryptophan-to-heme electron transfer in myoglobin revealed by UV 2D spectroscopy, *Science* **339**, 1586 (2013).
- [4] F. Calegari, D. Ayuso, A. Trabattoni, L. Belshaw, S. De Camillis, S. Anumula, F. Frassetto, L. Poletto, A. Palacios, P. Decleva, J. B. Greenwood, F. Martn, and M. Nisoli, Ultrafast electron dynamics in phenylalanine initiated by attosecond pulses, *Science* **346**, 336 (2014).
- [5] S. Beaulieu, A. Comby, D. Descamps, B. Fabre, G. A. Garcia, R. Gneaux, A. G. Harvey, F. Lgar, Z. Man, L. Nahon, A. F. Ordonez, S. Petit, B. Pons, Y. Mairesse, O. Smirnova, and V. Blanchet, Photoexcitation circular dichroism in chiral molecules, *Nat. Phys.* **14**, 484 (2018).
- [6] G. D. Scholes, G. R. Fleming, L. X. Chen, A. Aspuru-Guzik, A. Buchleitner, D. F. Coker, G. S. Engel, R. van Grondelle, A. Ishizaki, D. M. Jonas, J. S. Lundeen, J. K. McCusker, S. Mukamel, J. P. Ogilvie, A. Olaya-Castro, M. A. Ratner, F. C. Spano, K. B. Whaley, and X. Zhu, Using coherence to enhance function in chemical and biophysical systems, *Nature (London)* **543**, 647 (2017).
- [7] H. Lee, Y.-C. Cheng, and G. R. Fleming, Coherence dynamics in photosynthesis: Protein protection of excitonic coherence, *Science* **316**, 1462 (2007).
- [8] E. Collini, C. Y. Wong, K. E. Wilk, P. M. G. Curmi, P. Brumer, and G. D. Scholes, Coherently wired light-harvesting in photosynthetic marine algae at ambient temperature, *Nature (London)* **463**, 644 (2010).
- [9] F. D. Fuller, J. Pan, A. Gelzinis, V. Butkus, S. S. Senlik, D. E. Wilcox, C. F. Yocum, L. Valkunas, D. Abramavicius, and J. P. Ogilvie, Vibronic coherence in oxygenic photosynthesis, *Nat. Chem.* **6**, 706 (2014).
- [10] S. M. Falke, C. A. Rozzi, D. Brida, M. Maiuri, M. Amato, E. Sommer, A. D. Sio, A. Rubio, G. Cerullo, E. Molinari, and C. Lienau, Coherent ultrafast charge transfer in an organic photovoltaic blend, *Science* **344**, 1001 (2014).
- [11] M. Park, A. J. Neukirch, S. E. Reyes-Lillo, M. Lai, S. R. Ellis, D. Dietze, J. B. Neaton, P. Yang, S. Tretiak, and R. A. Mathies, Excited-state vibrational dynamics toward the polaron in methylammonium lead iodide perovskite, *Nat. Commun.* **9**, 2525 (2018).
- [12] G. Batignani, G. Fumero, A. R. S. Kandada, G. Cerullo, M. Gandini, C. Ferrante, A. Petrozza, and T. Scopigno, Probing femtosecond lattice displacement upon photo-carrier generation in lead halide perovskite, *Nat. Commun.* **9**, 1971 (2018).
- [13] A. Stolow, A. E. Bragg, and D. M. Neumark, Femtosecond time-resolved photoelectron spectroscopy, *Chem. Rev.* **104**, 1719 (2004).
- [14] I. V. Hertel and W. Radloff, Ultrafast dynamics in isolated molecules and molecular clusters, *Rep. Prog. Phys.* **69**, 1897 (2006).
- [15] V. E. Bondybey, Laser-induced fluorescence and bonding of metal dimers, *Science* **227**, 125 (1985).
- [16] Q. Liu, C. Wan, and A. H. Zewail, Solvation ultrafast dynamics of reactions. 13. Theoretical and experimental studies of wave packet reaction coherence and its density dependence, *J. Chem. Phys.* **100**, 18666 (1996).
- [17] M. Gühr, M. Bargheer, M. Fushitani, T. Kiljunen, and N. Schwentner, Ultrafast dynamics of halogens in rare gas solids, *Phys. Chem. Chem. Phys.* **9**, 779 (2007).
- [18] J. P. Toennies and A. F. Vilesov, Superfluid helium droplets: A uniquely cold nanomatrix for molecules and molecular complexes, *Angew. Chem. Int. Ed.* **43**, 2622 (2004).
- [19] C. Calegari and W. E. Ernst, Helium droplets as nanocryostats for molecular spectroscopy—from the vacuum ultraviolet to the microwave regime, in *Handbook of High Resolution Spectroscopy*, edited by F. Merkt and M. Quack (John Wiley & Sons, Chichester, 2011).

- [20] J. Higgins, C. Callegari, J. Reho, F. Stienkemeier, W. E. Ernst, K. K. Lehmann, M. Gutowski, and G. Scoles, Photo-induced chemical dynamics of high-spin alkali trimers, *Science* **273**, 629 (1996).
- [21] K. Nauta and R. E. Miller, Nonequilibrium self-assembly of long chains of polar molecules in superfluid helium, *Science* **283**, 1895 (1999).
- [22] K. Nauta and R. E. Miller, Metastable vibrationally excited HF ($v = 1$) in helium nanodroplets, *J. Chem. Phys.* **113**, 9466 (2000).
- [23] G. Haberfehlner, P. Thaler, D. Knez, A. Volk, F. Hofer, W. E. Ernst, and G. Kothleitner, Formation of bimetallic clusters in superfluid helium nanodroplets analysed by atomic resolution electron tomography, *Nat. Commun.* **6**, 8779 (2015).
- [24] J. Küpper and J. M. Merritt, Spectroscopy of free radicals and radical containing entrance-channel complexes in superfluid helium nanodroplets, *Int. Rev. Phys. Chem.* **26**, 249 (2007).
- [25] A. Gutberlet, G. Schwaab, Ö. Birer, M. Masia, A. Kaczmarek, H. Forbert, M. Havenith, and D. Marx, Aggregation-induced dissociation of HCl (H_2O)₄ below 1 K: The smallest droplet of acid, *Science* **324**, 1545 (2009).
- [26] A. V. Benderskii, J. Eloranta, R. Zadoyan, and V. A. Apkarian, A direct interrogation of superfluidity on molecular scales, *J. Chem. Phys.* **117**, 1201 (2002).
- [27] M. P. Ziemkiewicz, D. M. Neumark, and O. Gessner, Ultrafast electronic dynamics in helium nanodroplets, *Int. Rev. Phys. Chem.* **34**, 239 (2015).
- [28] M. Mudrich and F. Stienkemeier, Photoionisation of pure and doped helium nanodroplets, *Int. Rev. Phys. Chem.* **33**, 301 (2014).
- [29] J. von Vangerow, F. Coppens, A. Leal, M. Pi, M. Barranco, N. Halberstadt, F. Stienkemeier, and M. Mudrich, Imaging excited-state dynamics of doped He nanodroplets in real-time, *J. Chem. Phys. Lett.* **8**, 307 (2017).
- [30] L. Bruder, U. Bangert, M. Binz, D. Uhl, R. Vexiau, N. Bouloufa-Maafa, O. Dulieu, and F. Stienkemeier, Coherent multidimensional spectroscopy of dilute gas-phase nanosystems, *Nat. Commun.* **9**, 4823 (2018).
- [31] A. S. Chatterley, L. Schouder, L. Christiansen, B. Shepperson, M. H. Rasmussen, and H. Stapelfeldt, Long-lasting field-free alignment of large molecules inside helium nanodroplets, *Nat. Commun.* **10**, 133 (2019).
- [32] B. Shepperson, A. A. Søndergaard, L. Christiansen, J. Kaczmarczyk, R. E. Zillich, M. Lemeshko, and H. Stapelfeldt, Laser-Induced Rotation of Iodine Molecules in Helium Nanodroplets: Revivals and Breaking Free, *Phys. Rev. Lett.* **118**, 203203 (2017).
- [33] M. Mudrich, P. Heister, T. Hippler, C. Giese, O. Dulieu, and F. Stienkemeier, Spectroscopy of triplet states of Rb_2 by femtosecond pump-probe photoionization of doped helium nanodroplets, *Phys. Rev. A* **80**, 042512 (2009).
- [34] B. Grüner, M. Schlesinger, P. Heister, W. T. Strunz, F. Stienkemeier, and M. Mudrich, Vibrational relaxation and dephasing of Rb_2 attached to helium nanodroplets, *Phys. Chem. Chem. Phys.* **13**, 6816 (2011).
- [35] M. Schlesinger, M. Mudrich, F. Stienkemeier, and W. T. Strunz, Dissipative vibrational wave packet dynamics of alkali dimers attached to helium nanodroplets, *Chem. Phys. Lett.* **490**, 245 (2010).
- [36] H. Schmidt, J. von Vangerow, F. Stienkemeier, A. S. Bogomolov, A. V. Baklanov, D. M. Reich, W. Skomorowski, C. P. Koch, and M. Mudrich, Predissociation dynamics of lithium iodide, *J. Chem. Phys.* **142**, 044303 (2015).
- [37] B. Thaler, S. Ranftl, P. Heim, S. Cesnik, L. Treiber, R. Meyer, A. W. Hauser, W. E. Ernst, and M. Koch, Femtosecond photoexcitation dynamics inside a quantum solvent, *Nat. Commun.* **9**, 4006 (2018).
- [38] B. Thaler, R. Meyer, P. Heim, S. Ranftl, J. V. Pototschnig, A. W. Hauser, M. Koch, and W. E. Ernst, Conservation of hot thermal spin-orbit population of ^{23}P atoms in a cold quantum fluid environment, *J. Chem. Phys. A* **123**, 3977 (2019).
- [39] See Supplemental Material at <http://link.aps.org/supplemental/10.1103/PhysRevLett.124.115301>, which includes Refs. [40–45], for the assignment of the In_2 $\text{B}^3\Pi_g \leftarrow \text{X}^3\Pi_u$ band, measurements excluding a free dimer background, details on the sliding window Fourier analysis, and the 3/2 revival.
- [40] M. Douglas, R. Hauge, and J. Margrave, Electronic adsorption spectra of the group 3a metal dimers isolated in cryogenic matrixes, *J. Chem. Phys.* **87**, 2945 (1983).
- [41] P. Bicchi, C. Marinelli, and R. Bernheim, Electronic spectral transitions in In_2 , *J. Chem. Phys.* **97**, 8809 (1992).
- [42] A. Przystawik, S. Göde, T. Döppner, J. Tiggesbäumker, and K.-H. Meiwes-Broer, Light-induced collapse of metastable magnesium complexes formed in helium nanodroplets, *Phys. Rev. A* **78**, 021202(R) (2008).
- [43] A. Hernando, M. Barranco, R. Mayol, M. Pi, and F. Ancilotto, Density functional theory of the structure of magnesium-doped helium nanodroplets, *Phys. Rev. B* **78**, 184515 (2008).
- [44] M. J. J. Vrakking, D. M. Villeneuve, and A. Stolow, Observation of fractional revivals of a molecular wave packet, *Phys. Rev. A* **54**, R37 (1996).
- [45] M. Gühr, Coherent Dynamics of Small Molecules in Rare Gas Crystals (Cuvillier Verlag, Göttingen, 2005).
- [46] K. Balasubramanian and J. Li, Spectroscopic properties and potential energy surfaces of In_2 , *J. Chem. Phys.* **88**, 4979 (1988).
- [47] M. Bargheer, M. Gühr, and N. Schwentner, Collisions transfer coherence, *Isr. J. Chem.* **44**, 9 (2004).
- [48] F. Stienkemeier and K. K. Lehmann, Spectroscopy and dynamics in helium nanodroplets, *J. Phys. B* **39**, R127 (2006).
- [49] A. Vilá, M. Paniagua, and M. González, Vibrational energy relaxation dynamics of diatomic molecules inside superfluid helium nanodroplets. the case of the I_2 molecule, *Phys. Chem. Chem. Phys.* **20**, 118 (2018).
- [50] R. Monni, G. Auböck, D. Kinschel, K. M. Aziz-Lange, H. B. Gray, A. Vlek, and M. Chergui, Conservation of vibrational coherence in ultrafast electronic relaxation: The case of diplatinum complexes in solution, *Chem. Phys. Lett.* **683**, 112 (2017);
- [51] M. Renzler, M. Daxner, L. Kranabetter, A. Kaiser, A. W. Hauser, W. E. Ernst, A. Lindinger, R. Zillich, P. Scheier, and A. M. Ellis, Communication: Dopant-induced solvation of alkalis in liquid helium nanodroplets, *J. Chem. Phys.* **145**, 181101 (2016).